Materials Letters 93 (2013) 326–329

Contents lists available at SciVerse ScienceDirect

Materials Letters

journal homepage: www.elsevier.com/locate/matlet

Growth and electron field-emission of single-crystalline ZnO nanowires

Edgar Mosquera [a,*], Jimmy Bernal [a], Ramón A. Zarate [b], Frank Mendoza [c], Ram S. Katiyar [c], Gerardo Morell [c]

[a] Laboratorio de Materiales a Nanoescala, Departamento de Ciencia de los Materiales, Facultad de Ciencias Físicas y Matemáticas, Universidad de Chile, Av. Tupper 2069, Santiago, Chile
[b] Departamento de Física, Facultad de Ciencias, Universidad Católica del Norte, Casilla 1280, Antofagasta, Chile
[c] Department of Physics and Institute for Functional Nanomaterials, University of Puerto Rico, San Juan, PR 00931-3343, USA

ARTICLE INFO

Article history:
Received 22 August 2012
Accepted 27 November 2012
Available online 5 December 2012

Keywords:
Nanowires
High resolution TEM and FTT pattern
Structural characterization
Electron field emission

ABSTRACT

ZnO nanowires with high density are grown over zinc foil by thermal evaporation process at relatively low temperature. Electron microscopy studies confirmed that the as-grown nanowires are of single crystal hexagonal wurtzite structure, growing preferentially in the *c*-axis direction. The Raman spectrum of the ZnO nanowires shows an optical-phonon E_2 mode at 440 cm^{-1} confirming good crystallinity for the grown nanowires. The field emission measurement indicated that ZnO nanowires have a turn-on field of 9.1 V/μm at current density of 0.001 μA/cm^2.

© 2012 Elsevier B.V. All rights reserved.

1. Introduction

One-dimensional (1D) nanostructures such as nanowires, nanorods, nanobelts, nanoribbons and nanotubes have received considerable interest due to potential applications in electro-optical devices [1–7]. Among various 1D nanostructural materials, zinc oxide (ZnO) generates great interest for its direct wide band gap in the near ultraviolet range of 3.37 eV at room temperature (RT), large exciton with binding energy of 60 meV versus 25 meV for GaN, and stable chemical and physical properties. Recently, ZnO nanostructures have been synthesized by several methods [8], among which the vapor transport and deposition method is most commonly used. However, such method often uses catalysts or other additives to assist and control the growth process [9–11]. Contrary, some catalyst-free methods such as thermal annealing have been reported to synthesize 1D ZnO nanostructures via a self-catalysis process of ZnO [12–15]. This method has the virtue of simplicity, efficiency, and low cost, which facilitates the synthesis of nanowires in one step without templates.

In this article, we report the formation of single-crystalline and dense array of 1D ZnO nanowires directly grown on Zn foil under air ambient at 550 °C without employing any metal catalytic. The obtained nanowires were grown preferentially in the *c*-axis direction on the zinc foil. Structural properties of the prepared ZnO nanowires have been confirmed using electron microscopy and Raman spectroscopy. Field emission measurements results reveal that the ZnO nanowires arrays possess efficient field emission.

2. Experimental details

Preparation of samples: The experimental setup is described in Ref. [13]. Zinc foils (15 mm × 15 mm × 0.2 mm) with purity of 99.9% were carefully cleaned with absolute isopropyl alcohol in an ultrasonic bath (53 kHz) for 30 min. After evaporation of isopropyl alcohol in air, the substrate was loaded onto an optical borosilicate glass substrate (22 mm × 70 mm) and loaded into a quartz tube. The glass substrate was positioned in the middle of the quartz tube and also the middle of the tube furnace. For all experiments the furnace was heated at the rate of 10 °C min^{-1} to a designed temperature. The temperature was maintained for 1 h and finally the system was cooled naturally to room temperature.

Characterization: Scanning Electron Microscopy (SEM) images were obtained using a Carl Zeiss EVO MA 10 model operating at an accelerating voltage of 10 kV. The best-grown sample was characterized by a Tecnai F20 FEG-S/TEM operated at 200 kV, equipped with an EDX detector. The TEM samples were ultrasonically dispersed in isopropyl alcohol and then collected in an ultrathin holey carbon-coated Cu grid. Raman spectra were recorded at room temperature in a backscattering geometry using a triple monochromator Jobin-Yvon Inc. T64000 Raman spectrometer; the spectral resolution is 1 cm^{-1}. Radiation at 514.5 nm (2.41 eV) from a Coherent Innova 99 Ar^+ laser was focused on the sample using an 80× objective, and the probe area was of 1–2 μm in diameter. The power on the sample was kept below 10 mW to avoid damage.

* Corresponding author. Tel.: +56 2 978 4795/978 4222; fax: +56 2 699 4119.
E-mail address: edemova@ing.uchile.cl (E. Mosquera).

0167-577X/$ - see front matter © 2012 Elsevier B.V. All rights reserved.
http://dx.doi.org/10.1016/j.matlet.2012.11.119

Field emission I–V characteristics were measured in a custom made system, described in detail elsewhere [16]. Briefly, a diode configuration is used, in which a molybdenum rod of 3 mm diameter (area: 0.071 cm^2) serves as an anode. Voltage is applied using a Stanford Research Systems PS350 power supply. The emitted current is measured with a Keithley 6517A electrometer. For the configuration employed, macroscopic surface electric field (E_S) on the sample (i.e. cathode) can be estimated accurately by $E_S = V/d_{CA}$, where V is the voltage applied to the anode and d_{CA} is the distance between the anode and the cathode [17]. All the measurements were taken at $d_{CA} = 100 \pm 2$ mm, and at a pressure of $1\text{–}2 \times 10^{-7}$ Torr ($1.3 - 2.7 \times 10^{-7}$ mbar). Currents lower than 1×10^{-12} A were considered at the background noise level. The current density was calculated by dividing the current over the area of the sample subjected to $E_S = V/d_{CA}$, which, in our specific configuration, is well approximated by using the area of the anode (0.071 cm^2) [16]. The turn-on field (E_t) was defined as the electric field necessary to emit a current density of 10 μA/cm^2. Each data point in the I–V curves is the average of 8 measurements taken 250 ms apart. For data acquisition, a custom Lab View (National Instruments) program was developed. As a measure of precaution to avoid the influence of displacement or charging current in the field-emitted current, specifically in currents smaller than 1×10^{-11} A, a delay of 4 s between the change in voltage and the data acquisition was employed.

3. Results and discussion

Fig. 1(a) and (b) shows the typical TEM images of the grown nanostructures obtained by thermal evaporation process in air atmosphere. These images clearly reveal that the formed products are nanowires and grown over the entire zinc foil substrate in a high density. It is observed that the nanowires are randomly grown and partially aligned to the surface. Typical diameters of the grown nanowires at 550 °C are ~50 nm. Typical lengths of the obtained nanowires are in the range of 10–30 μm. The highest temperature of 550 °C allowed obtaining a higher density of nanowires; therefore the temperature of 550 °C was found to be the optimum temperature for the growth of dense nanowires. However, it is well known that ZnO nanowires could be grown effectively on the Zn foil substrate at a relatively low temperature [2,15]. We investigated the initial nucleation of ZnO nanowires at low temperatures for a very short duration of 30 min at 450 °C. Here, we observed that it was necessary to increase the time to 1 h to obtain the formation of a dense layer of ZnO nanowires. This short duration of 30 min and low temperature clearly demonstrates the critical effect of temperature on the growth.

Several studies have been done on the synthesis of ZnO nanowires by thermal evaporation of Zn like microspheres and powders in different oxidizing atmospheres [9–15]. However, in our study we have found that annealing the Zn foil without catalyst microparticles in air atmosphere gives optimum growth of nanowires, and very thin nanowires compared with literature [18–23]. Here we kept the Zn foil into the furnace from the beginning of the experiment in air atmosphere; hence, we believe that a small layer of ZnO could be already formed before the melting point of metallic zinc (m.p. of Zn = 419 °C) was reached. In our case the oxygen can easily diffuse through the zinc foil, which can explain the growth of long nanowires in such a short time.

Further structural characterization of the ZnO nanowires was performed by high-resolution (HR) TEM. Fig. 2 shows the crystalline nature of the ZnO nanowire. The lattice spacing calculated from the results reveals 0.52 nm, which is in an excellent agreement with the lattice constant of single-crystalline ZnO. The lattice spacing of 0.52 nm corresponds to preferred growth orientation (0001) crystal planes along the c-axis, further confirming that ⟨0001⟩ is the preferential growth direction of these wurtzite-type ZnO nanowires. The FFT pattern shown in Fig. 2 (inset) reveals a well defined and ordered diffraction pattern indicating very high crystallinity with the c-axis growth direction of the grown ZnO nanowires. Fig. 2b shows the formation of thin amorphous carbon layer produced during the electron irradiation in TEM mode.

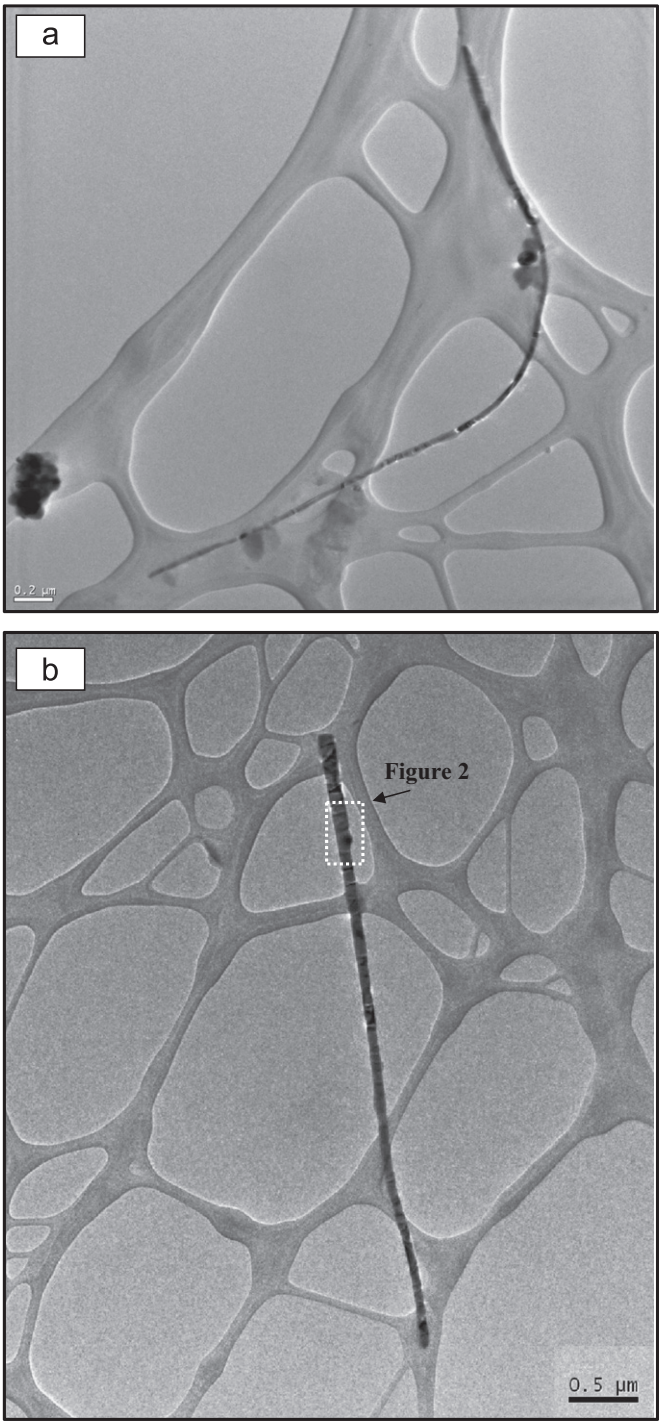

Fig. 1. (a and b) Low magnified TEM images of two ZnO nanowires. The doted frame in (b) is shown in Fig. 2.

Raman scattering was performed to investigate vibrational properties of the ZnO nanowires produced at 550 °C for 1 h. ZnO with hexagonal wurtzite structure belongs to the C^4_{6v} space

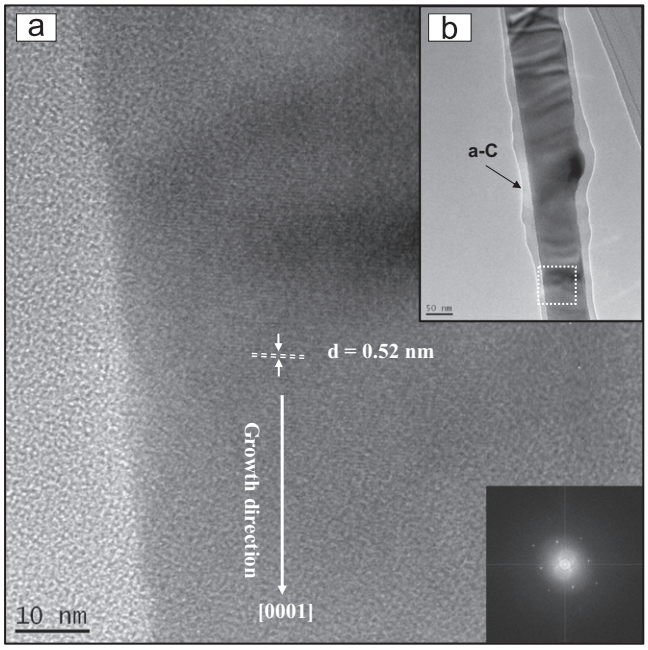

Fig. 2. (a) High-resolution TEM image of ZnO nanowire showing its [0001] growth direction. The dotted frame in (b) is shown magnified in (a) to reveal the crystalline nature of the nanowires. Inset FFT pattern.

group having two formula units per primitive cell. According to group theory, single-crystalline ZnO has eight sets of optical phonon modes at Γ point of the Brillouin zone, classified as $A_1+E_1+2E_2$ modes (Raman active), $2B_1$ modes (Raman silent) and A_1+E_1 modes (infrared active). Moreover, the A_1 and E_1 modes split into transverse-optical (TO) and longitudinal-optical (LO) phonons [15,24]. The measured Raman spectra of ZnO bulk (bottom) and nanowires (top) samples are shown in Fig. 3. In the nanowires spectrum (Fig. 3(b)), the peak at 440 cm^{-1} corresponds to E_2 (high), which is shifted by 2 cm^{-1} compared to bulk. E_2 (high) is usually used to analyze the stress state in films due to its high sensitivity to stress. An increase in the E_2 phonon frequency is ascribed to compressive stress, whereas a decrease in the E_2 phonon frequency is ascribed to tensile stress [25]. The blue shift of the E_2 mode corresponding to the 438 cm^{-1} of the bulk ZnO demonstrated that possibly the ZnO nanowires grown on the Zn foil substrate are under compressive stress, and also can be due to the local heating effects due to the synthesis condition of the samples [26,27]. The larger stress of our sample could be attributed to the more oxygen defects in the ZnO nanowires, but more oxygen vacancy will permit to have a higher intensity of the LO phonon of A_1 mode, which is around 575–580 cm^{-1} [28].

Dependence of the electron field emission current density on the applied electric field (J–E) of ZnO nanowires arrays is shown in Fig. 4. The turn-on field (the field required to produce current density of 10 $\mu A/cm^2$) was 9.1 V/μm at current density of 0.001 $\mu A/cm^2$ and a threshold field of 21 V/μm at current density of 0.1 mA/cm^2.

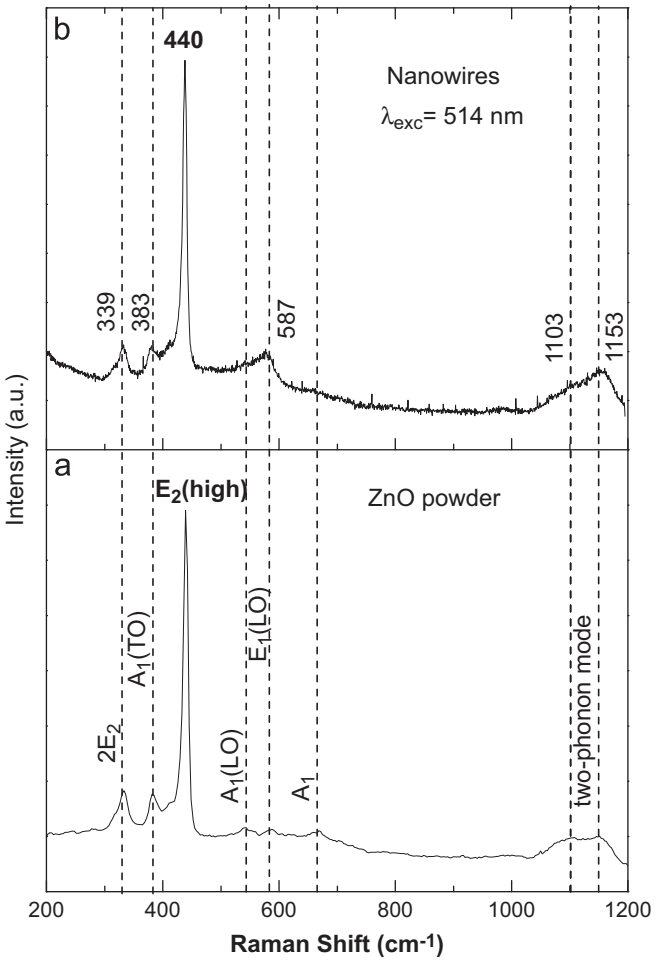

Fig. 3. Raman spectra of (a) bulk ZnO and ZnO nanowires excited at (b) 514.5 nm.

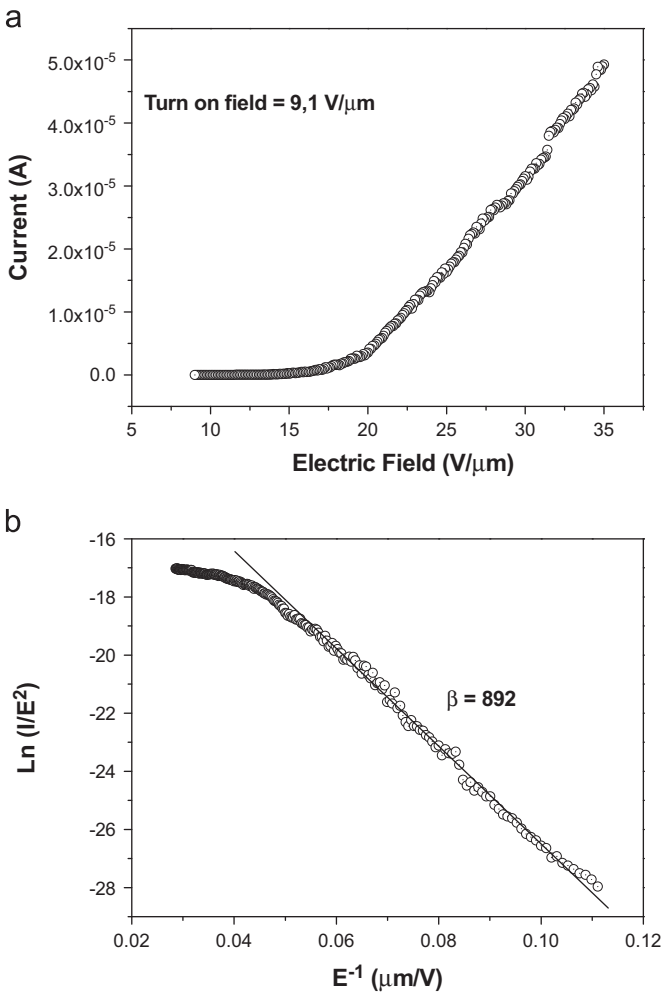

Fig. 4. (a) Field emission current on the applied electric field ((*I*–*E*) of ZnO nanowires). (b) Fowler–Nordheim plot.

In order to investigate the field emission behavior, $\ln(I/E^2)$ and I/E is also analyzed according to the Fowler–Nordhein (F–N) equation:

$$J = A\left(\beta^2 E^2/\phi\right) exp\left(-B\phi^{3/2}/\beta E\right) \quad (1)$$

where $A = 1.54 \times 10^{-10}\,\mathrm{A\,V^{-2}\,eV}$ and $B = 6.82 \times 10^{9}\,\mathrm{V/(eV^{3/2}\,m)}$ are constants, and ϕ is the work function of the emitter (eV). β is the field enhancement factor of the ZnO nanowires, which is estimated to be 892 from the averaged slope of the F–N plot under assumption of a work function of 5.3 eV from ZnO emmiter [1,11,15]. Fig. 4(b) presents the F–N plot, which is good enough for various applications in field-emission microelectronic devices.

It is very important to note that the length distribution of the nanowires is not uniform with respect to their heights, therefore it is very difficult to determine the areas that are really responsible for the field emission. However, we think that when the applied electric field is low, the nanowires that only have relatively higher heights are active in the field emission process. But when the electric field becomes higher, more area of the nanostructures can contribute to the emission current. For this reason, the possible effects of aspect ratio and emission site density on the field emission devices could not be explained explicitly.

4. Summary

ZnO nanowires with hexagonal wurtzite structure have been grown on zinc foil by using a simple evaporation thermal method in air atmosphere for 1 h. Typical diameters of the grown nanowires at 550 °C are ~50 nm. The Raman spectrum of ZnO nanowires reveals good crystal quality and a higher-order Raman process. The electron field emission characterization from the wires was also investigated. The turn-on voltage for ZnO nanowires was found to be about 9.1 V/μm at a current density of 0.001 $\mu A/cm^2$.

Acknowledgments

This work has been partially financed by FONDECYT Grant no. 11110001 and has benefited from access to equipments from the Facultad de Ciencias Físicas y Matemáticas of the Universidad de Chile, and from the University of Puerto Rico, Rio Piedras Campus.

References

[1] Yongai Z, Chaoxing W, Yong Z, Tailiang G. J Semicond 2012;33:023001-1–5.
[2] Wen X, Fang Y, Pang Q, Yang C, Wang J, Ge W, et al. J Phys Chem B 2005;109:15303–8.
[3] Zhu G, Zhou Y, Wang S, Yang R, Ding Y, Wang X, et al. Nanotechnology 2012;23:055604-1–6.
[4] Wang X, Ding Y, Summers CJ, Wang ZL. J Phys Chem B 2004;108:8773–7.
[5] Xia Y, Yang P, Sun Y, Wu Y, Mayers B, Gates B, et al. Adv Mater 2003;15:353–89.
[6] Li JY, Chen XL, Li H, He M, Qiao ZY. J Cryst Growth 2001;233:5–7.
[7] Samanta PK, Chaudhuri. PR. Sci Adv Mater 2011;3:107–12.
[8] Chen H, Wu X, Gong L, Ye C, Qu F, Shen G. Nanoscale Res Lett 2010;5:570–5.
[9] Zhu Z, Chen TL, Gu Y, Warren J, Osgood RM. Chem Mater 2005;17:4227–34.
[10] Lyu SC, Zhang Y, Lee CJ, Ruh H, Lee HJ. Chem Mater 2003;15:3294–9.
[11] Tseng YK, Huang CJ, Cheng HM, Lin IN, Liu KS, Chen IC. Adv Funct Mater 2003;13:811–4.
[12] Liu Y, Chen Z, Kang Z, Bello I, Fan X, Shafiq I, et al. J Phys Chem C 2008;112:9214–8.
[13] Mosquera E, Bernal J, Morel M, Zarate RA. J Nanoeng Nanomanuf 2012;2:253–8.
[14] Zhang X, Wang L, Zhou G. Rev Adv Mater Sci 2005;10:69–72.
[15] Ghoshal T, Biswas S, Kar S, Dev A, Chakrabarti S, Chaudhuri S. Nanotechnology 2008;19:065606-1–065606-11.
[16] Morell G, Berríos AG, Weiner BR, Gupta SJ. J. Mater Sci 2006;17:443–51.
[17] Berríos AG, Piazza F, Morell G. J Vac Sci Technol B 2005;23:645–8.
[18] Yang R, Wang ZL. Solid State Commun 2005;134:741–5.
[19] Sekar A, Kim SH, Umar A, Hahn YB. J Cryst Growth 2005;277:471–8.
[20] Umar A, Kim SH, Lee YS, Nahm KS, Hahn YB. J Cryst Growth 2005;282:131–6.
[21] Dang HY, Wang J, Fan SS. Nanotechnology 2003;14:738–41.
[22] Fan HJ, Scholz R, Kolb FM, Zacharias M. Appl Phys Lett 2004;85:4142–4.
[23] Yu W, Pan C. Mater Chem Phys 2009;115:74–9.
[24] Dament TC, Porto SPS, Tell B. Phys Rev 1996;142:570–4.
[25] Triphaty S, Chua SJ, Chen P, Miao ZL. J Appl Phys 2002;92:3503–10.
[26] Alim KA, Fonoberov VA, Shamsa M, Balandin AA. J Appl Phys 2005;97:124313–5.
[27] Rajalakshmi M, Arora AK, Bendre BS, Mahamuni S. J Appl Phys 2000;87:2445–8.
[28] Umar A, Kim SH, Kim JH, Park YK, Hahn YB. Mater Lett 2007;61:4954–8.